

Survey of QCD spectral sum rules

QCD spectral sum rules are different versions and/or improvements of the previous Hilbert representation in Eq. (48.2). For the purposes of more general discussions, let us forget QCD for the moment, namely the theoretical side $\text{Re } \Pi(q^2)$, and we shall concentrate on the RHS spectral integral.

In some channels such as $e^+e^- \rightarrow \text{hadrons}$ or $\tau \rightarrow \nu_\tau + \text{hadrons}$ data, the spectral function $\text{Im}\Pi(t)$ is known from the data, and the sum rules can be used for determining the QCD parameters given in Tables 48.1 and 48.2. In other channels, the sum rules are used for determining the properties of the hadrons for a guide to their experimental searches. In this case, one has to introduce a model for parametrizing the spectral function. For this purpose, the most common model used in the sum rule analysis is the so-called *naïve duality ansatz*, where the spectral function reads:

$$\text{Im}\Pi(t) = f_H^2 M_H^{2d} \delta(t - M_H^2) + \theta(t - t_c) \text{Im}\Pi_{\text{QCD}}(t). \quad (49.1)$$

f_H is the coupling having the dimension of mass of the lowest hadron ground state H to the hadronic current; d is the power of t in the asymptotic t -behaviour of the spectral function ($d = 0$ for the vector two-point function, ...); t_c is the ‘QCD continuum’ threshold above which the spectral function is approximated by the discontinuity $\text{Im}\Pi_{\text{QCD}}(t)$ of the QCD diagram, which is expected to smear the contributions of the higher mass radial excitations. We shall test later on in some examples the accuracy of this simple duality ansatz for reproducing the measured spectral function.

An alternative parametrization can be provided by approximating the spectral function with an infinite sum of narrow resonances:

$$\text{Im}\Pi(t) = \sum_H f_H^2 M_H^2 \delta(t - M_H^2), \quad (49.2)$$

where the model is supported by the large N_c -behaviour of QCD as discussed in the previous part of this book.

49.1 Moment sum rules in QCD

In QCD the number of derivatives required to obtain a well-defined two-point function is fixed by the asymptotic freedom property of the theory. For a gauge-invariant local operator

$J_H(x)$, the asymptotic behaviour of the associated two-point function is of the type:

$$\lim_{t \rightarrow \infty} \frac{1}{\pi} \text{Im}\Pi(t) \sim A t^d \left\{ 1 + a_1 \frac{\alpha_s(t)}{\pi} + \dots \right\}, \quad (49.3)$$

with A and a_1 calculable coefficients, and d a known integer $d = 0, 1, 2, \dots$, depending on the dimensions of the operator $J_H(x)$. It is then sufficient to take $d + 1$ derivatives with respect to q^2 to get rid of the arbitrary polynomial and obtain a convergent integral. The functions defined by the *moment integrals* ($Q^2 \equiv -q^2$):

$$\begin{aligned} \Pi^{(m)}(Q^2) &= \frac{(-1)^m}{(m-d-1)!} (Q^2)^{m-d} \frac{\partial^m}{(\partial Q^2)^m} \Pi(q^2) \\ &= \int_0^\infty dt \frac{m(m-1)\cdots(m-d)}{(t+Q^2)^{d+1}} \left(\frac{Q^2}{t+Q^2} \right)^{m-d} \frac{1}{\pi} \text{Im}\Pi(t), \end{aligned} \quad (49.4)$$

for $m \geq d + 1$ are then well-defined functions calculable in perturbative QCD at sufficiently large Q^2 -values. To our knowledge, these sum rules were first discussed by Yndurain [631] in connection with the study of $e^+e^- \rightarrow$ hadrons data and used later on for heavy-quark systems [632,1,434]. One can notice that for high-derivative moments, the rôle of the ground state is enhanced in the sum rule. Therefore the sum rule in Eq. (49.4) is a good candidate for studying the low-energy properties of hadrons as we shall see later on.

A classical example of moments sum rules is the D -function defined in Eq. (33.20), which is superconvergent and therefore obeys an homogeneous RGE. From Eq. (33.25), one can deduce for three massless flavours:

$$\begin{aligned} D(Q^2) &\equiv -Q^2 \frac{d}{dQ^2} \Pi_{\text{em}}(Q^2) = \int_0^\infty \frac{dt}{(t+Q^2)^2} \frac{1}{\pi} \text{Im}\Pi_{\text{em}}(t) \\ &= \frac{2}{16\pi^2} \left[1 + \left(\frac{\bar{\alpha}_s}{\pi} \right) + 1.64 \left(\frac{\bar{\alpha}_s}{\pi} \right)^2 + 6.37 \left(\frac{\bar{\alpha}_s}{\pi} \right)^3 + \dots + \text{non-perturbative} \right]. \end{aligned} \quad (49.5)$$

However, when trying to confront this sum rule with experiment, there appears the problem that the integrand in the RHS is only known experimentally from the threshold up to finite values of t . This brings in a question of *matching* whatever is known about the low-energy hadronic spectral function with its asymptotic behaviour as predicted by pQCD.

49.2 Laplace sum rule (LSR)

This type of sum rule is derived from the previous dispersion relation in Eq. (48.2) by applying to both sides the *inverse Laplace operator* [1]:¹ ($Q^2 \equiv -q^2 \geq 0$):

$$\hat{\mathcal{L}} \equiv \lim_{n, Q^2 \rightarrow \infty} (-1)^n \frac{(Q^2)^n}{(n-1)!} \frac{\partial^n}{\partial Q^2^n}, \quad (49.6)$$

¹ This sum rule was originally called the Borel sum rule by SVZ [1].

where $n/Q^2 \equiv \tau$ is fixed, which is the Laplace sum rule variable. It has been found in the study of the radiative corrections that sum rule expression of these radiative terms naturally have the properties of the Laplace transform [626], whilst later on [405], it has also been noticed that the operator $\hat{\mathcal{L}}$ is an algebraic form of the Laplace inversion operator. These observations led to simplifications in the derivation of the QCD expressions of the sum rules once one knows the expression of the two-point correlator $\Pi(q^2)$. Useful expressions are collected in Appendix G. Therefore, one gets the exponential form of the sum rule:

$$\hat{\mathcal{L}}\Pi = \tau \int_0^\infty dt e^{-t\tau} \frac{1}{\pi} \text{Im}\Pi(t). \quad (49.7)$$

As can be seen in the derivation of the Laplace sum rule, one has to assume that various derivatives exist. For an approximate truncated series as in QCD improved by the renormalization group equation, this existence is satisfied as in the case of the moment sum rules. The advantages of $\hat{\mathcal{L}}\Pi$ are two-fold:

- First, the use of various derivatives helps to eliminate the subtraction terms in Eq. (48.2), which are often polynomials in q^2 .
- Second, the exponential factor increases the role of the ground state into the spectral integral if the QSSR variable τ is not too small, but still not too large for the perturbative calculation to make sense. In practice τ is about the value of the hadronic scale. This fact is welcome for low-energy physics.

49.3 Ratio of moments

From Eq. (49.7), one can derive the ratio of moments [91–93]:

$$R(\tau) = -\frac{d}{d\tau} \log \int_0^\infty dt e^{-t\tau} \frac{1}{\pi} \text{Im}\Pi(t), \quad (49.8)$$

or the finite energy-like [1]:

$$R_c(\tau) = \frac{\int_0^{t_c} dt t e^{-t\tau} \frac{1}{\pi} \text{Im}\Pi(t)}{\int_0^{t_c} dt e^{-t\tau} \frac{1}{\pi} \text{Im}\Pi(t)}. \quad (49.9)$$

Its non-relativistic version is obtained by transforming the variable t into the non-relativistic energy E and $\tau_N = 4m\tau$. In this way, the ratio becomes:

$$R(\tau_N) = -\frac{d}{d\tau_N} \log \int_0^\infty dE e^{-E\tau_N} \frac{1}{\pi} \text{Im}\Pi(t), \quad (49.10)$$

where τ_N can be interpreted as the *imaginary time* variable. The advantage of the ratio of moments can be explicitly seen in the following way:

- If one uses the simple duality ansatz ‘one resonance’ plus ‘QCD continuum’ for parametrizing the spectral function, one can see that the two sum rules in Eqs. (49.8) and (49.9) give an expression of the mass squared of the ground state. More precisely, for large τ values, the RHS of the sum rule tends to the mass squared of the lowest resonance.

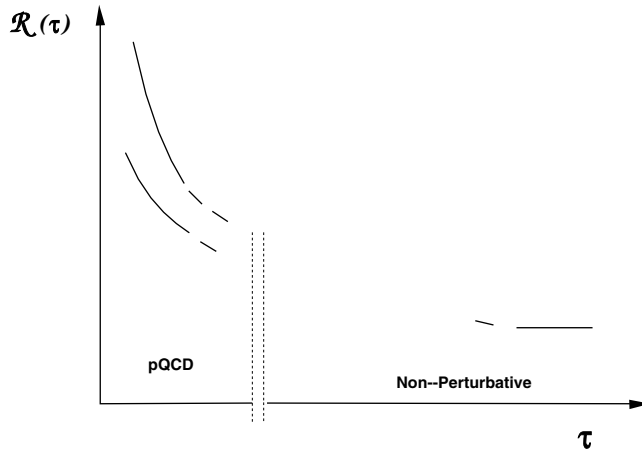


Fig. 49.1. Expected behaviour of $\mathcal{R}(\tau)$ at short and long distances.

- For small τ -values, the ratio of moments has the parton model behaviour:

$$\mathcal{R}(\tau) = (d + 1)\tau^{-1}[1 + \text{QCD corrections}] , \tag{49.11}$$

where d is the only reminiscence left from the number of subtractions needed in the dispersion relation for the initial two-point function. For large τ values, the ratio of moments is dominated by the non-perturbative corrections. In the *sum rule window* compromise region, where the moments stabilize, these non-perturbative corrections are small though vital for stabilizing the result. These features lead to the expected behaviour of \mathcal{R} given in Fig. 49.1.

- Because of the positivity property of a spectral function $\text{Im}\Pi(t) \geq 0$, the function $-\log \mathcal{M}(\tau)$ is a concave function of τ ; or in other words, the slope of the function $\mathcal{R}(\tau)$ must always be negative. This of course implies severe restrictions on the way that the two asymptotic regimes illustrated in Fig. 49.1 can be joined. The proof of this property is rather straightforward. It can be understood very simply by making an analogy with statistical mechanics: $\mathcal{R}(\tau)$ can be viewed as the equilibrium ‘energy’ $\langle t \rangle$ of a system with variable ‘energy’ t in thermal equilibrium with a second system at ‘temperature’ $1/\tau$. In this analogy, $\text{Im}\Pi(t)$ represents the ‘density of states’ with ‘energy’ t . Then the mean squared ‘energy fluctuation’ is given by:

$$-\frac{d}{d\tau} \mathcal{R}(\tau) \equiv \langle (t - \langle t \rangle)^2 \rangle = \langle t^2 \rangle - \langle t \rangle^2 \geq 0 , \tag{49.12}$$

which by definition is a positive quantity.

- In its non-relativistic version, the ratio of moments tends to the ground state energy E_0 for large imaginary time $\tau_N \rightarrow \infty$. In the corresponding theoretical perturbative expansion, the minimum of \mathcal{R} gives an approximation of this ground state energy:

$$\min \mathcal{R}(\tau_N) = E_0 , \tag{49.13}$$

and the mass of the ground state is given by:

$$M = 2m + \mathcal{R}(\tau_N) . \tag{49.14}$$

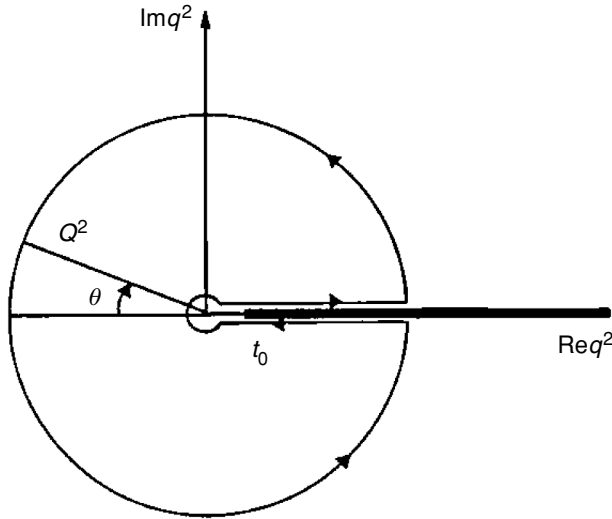


Fig. 49.2. Contour integral in the complex q^2 -plane, with $q^2 = -Q^2 \exp(i\theta)$.

49.4 Finite energy sum rule (FESR)

Another version of QSSR is the FESR:

$$\mathcal{M}_n(Q^2) \equiv \int_0^{Q^2} dt t^n \frac{1}{\pi} \text{Im}\Pi_{\text{QCD}}(t) \simeq \int_0^{Q^2} dt t^n \frac{1}{\pi} \text{Im}\Pi_{\text{exp}}(t) \quad : n = 0, 1, \dots, \tag{49.15}$$

which was known a long time before QCD [627]. The previous FESR can be derived in many ways. One way to derive the FESR is the use of the Cauchy theorem on a finite radius contour in the complex q^2 plane (Fig. 49.2) à la Shankar [628].

Avoiding the cut along the real axis, it leads to [628,28,31]:

$$\frac{1}{2\pi i} \oint dz z^n \Pi(z) = 0. \tag{49.16}$$

If one neglects the contribution of the little circle around the origin which is safer if $\Pi(0) = 0$, one deduces the moments:

$$\mathcal{M}_n(Q^2) = \int_0^{Q^2} dt t^n \frac{1}{\pi} \text{Im}\Pi(t) = (-1)^{n+1} \frac{(Q^2)^{n-1}}{2\pi} \cdot \int_{-\pi}^{+\pi} d\theta e^{i(n+1)\theta} \Pi(Q^2 e^{i\theta}), \tag{49.17}$$

where the LHS can be measured from the data and comes from the paths above and below the real axis which pick up the discontinuity of $\Pi(q^2)$ and then its imaginary part. The RHS comes from the big circle of radius Q^2 , which can be computed in QCD provided it is large enough. The sum rule results from the matching of these two contributions. However, as

the FESR diverges for increasing n , the real axis is dominated by the high Q^2 region. For the RHS to reproduce this correctly, more information on the behaviour of the two-point correlator in the region of the big circle near the cut is needed. This means that more and more non-leading terms in the series expansion become important at large n and can destroy the convergences of the series.

49.5 Features of FESR and an example

Now, let us return to the FESR in Eq. (49.15). Contrary to the LSR in Eq. (49.7), where the role of the lowest ground state is enhanced by the exponential factor, the FESR is governed by the effects of high-mass resonances; that is it needs a good control of the continuum contributions to the sum rule. In some cases, where a stability in t_c (continuum threshold) does not occur, this is a great disadvantage.

Taking the example of the isovector part of the electromagnetic current (the ρ -meson channel), one can show that FESR can provide a useful way for a correct matching between the low-energy hadronic spectral function and the onset of QCD perturbative continuum. In this sense, it complements the analysis from the LSR. Using the naïve duality ansatz for the hadronic spectral function, the spectral function reads:

$$\frac{1}{\pi} \text{Im}\Pi(t)_{I=1} = \frac{M_\rho^2}{4\gamma_\rho^2} \delta(t - M_\rho^2) + \frac{N_c}{16\pi^2} \frac{2}{3} \theta(t - t_c) [1 + \dots], \quad (49.18)$$

where the ρ -meson coupling $\gamma_\rho \simeq 2.55$ is normalized in Eq. (2.52). Using the $n = 0$ FESR moments, one can derive the constraint:

$$\frac{M_\rho^2}{4\gamma_\rho^2} \simeq \frac{N_c}{16\pi^2} \frac{2}{3} t_c [1 + \dots]. \quad (49.19)$$

Using the experimental values of the ρ -meson parameters, and adding QCD corrections, one obtains (see details in [405,3]):

$$t_c \simeq 1.7 \text{ GeV}^2, \quad (49.20)$$

which is reasonably high for pQCD calculation to make sense. It is worthwhile to notice that the FESR fixes both the lowest ground state parameters and the correlated value of the QCD continuum threshold t_c , as contrary to the LSR, the FESR is weighted by the high-energy region for positive values of the degree n of the moment. However in some cases, this property become a great inconvenience of the method.

In general, this value of t_c is slightly different from the phenomenological value of the first radial excitation mass. This might be not so surprising as the QCD model, which gives a smearing of the high-energy region, cannot take into account the complicated structure of the resonances in this region.

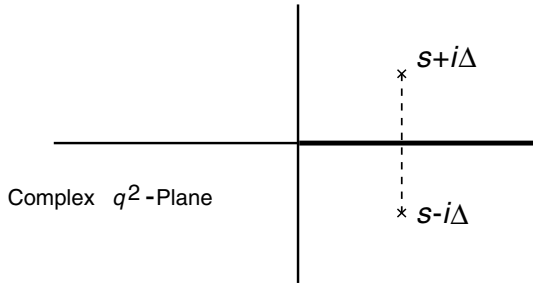


Fig. 49.3. Points in the complex q^2 -plane where the two-point function in Eq. (49.22) is evaluated.

49.6 The Gaussian sum rules

Another way of deriving the FESR which casts light upon the meaning of local duality is the Gaussian sum rule which reads [405,406]:

$$G(s, \sigma) = \frac{1}{\sqrt{4\pi\sigma}} \int_0^\infty dt e^{-\frac{(t+s)^2}{4\sigma}} \frac{1}{\pi} \text{Im}\Pi(t), \tag{49.21}$$

for a Gaussian centred at s with a finite width resolution $\sqrt{4\pi\sigma}$. Let us discuss how to get the Gaussian transform from a generic two-point function like $\Pi(q^2)$ in Eq. (48.1). First, one evaluates $\Pi(q^2)$ at a complex point $q^2 = s + i\Delta$ (s and Δ are real positive variables) and at its complex conjugate $q^2 = s - i\Delta$ (see Fig. 49.3) and defines the combination, (one assumes for simplicity that the dispersion relation for $\Pi(q^2)$ requires at most one subtraction, but the argument can be easily generalized as in the case discussed for the Laplace transform):

$$\frac{\Pi(s + i\Delta)}{i\Delta} + \frac{\Pi(s - i\Delta)}{-i\Delta} = \int_0^\infty dt \frac{1}{(t-s)^2 + \Delta^2} \frac{1}{\pi} \text{Im}\Pi(t). \tag{49.22}$$

The integral in the RHS brings in the convolution with a Lorentz-like kernel which we can write as a Laplace transform

$$\frac{1}{(t-s)^2 + \Delta^2} = \int_0^\infty dx e^{-x\Delta^2} e^{-x(t-s)^2}. \tag{49.23}$$

Applying the techniques developed in the previous Section 49.2 to this integral representation allows us to construct the inverse Laplace transform operator which is needed to obtain the Gaussian transform in Eq. (49.21) from the Lorentz transform in Eq. (48.2). It is the operator:

$$\mathbf{L} \equiv \lim_{N, \Delta^2 \rightarrow \infty} \Big|_{\frac{1}{N}\Delta^2=4\tau} \frac{(-1)^N}{(N-1)!} (\Delta^2)^N \frac{\partial^N}{(\partial\Delta^2)^N}. \tag{49.24}$$

We then have the desired relation:

$$\frac{1}{\sqrt{4\pi\tau}} 2\tau \mathbf{L} \left[\frac{\Pi(s + i\Delta)}{i\Delta} + \frac{\Pi(s - i\Delta)}{-i\Delta} \right] \tag{49.25}$$

$$\Rightarrow \frac{1}{\sqrt{4\pi\tau}} \int_0^\infty dt \exp\left(-\frac{(s-t)^2}{4\tau}\right) \frac{1}{\pi} \text{Im}\Pi(t). \quad (49.26)$$

One can also note that Eq. (49.21) can be derived by applying the inverse Laplace operator:

$$\hat{\mathcal{L}} \equiv \lim_{n, \tau^2 \rightarrow \infty} \frac{(-\tau^2)^n}{(n-1)!} \frac{d^n}{(d\tau^2)^n}, \quad (49.27)$$

where $n/\tau^2 \equiv \sigma$ is fixed, to the already Laplace-transformed quantity:

$$\mathcal{F}(\tau) = e^{-s\tau} \tau^{-1} \int_0^\infty dt e^{-t\tau} \frac{1}{\pi} \text{Im}\Pi(t). \quad (49.28)$$

One can already note from Eq. (49.21) that in limit $\sigma = 0$, where the Gaussian kernel becomes a delta function, one has the *strict local duality*:

$$G(s, 0) = \frac{1}{\pi} \text{Im}\Pi(s). \quad (49.29)$$

Also, Eq. (49.21) obeys the heat-evolution equation:

$$\left(\frac{\partial^2}{\partial s^2} - \frac{\partial}{\partial \sigma}\right) G(s, \sigma) = 0, \quad (49.30)$$

with the initial condition in Eq. (49.29), where now s is the position, σ the time evolution and $\frac{1}{\pi} \text{Im}\Pi(t)$ the temperature distribution in the region $0 \leq s \leq \infty$. The two boundary conditions for $\sigma > 0$:

$$G(s = 0, \sigma) = 0, \quad \frac{\partial G}{\partial s}(s, \sigma)|_{s=0} = 0, \quad (49.31)$$

lead to two independent solutions $U^-(s, \sigma)$ and $U^+(s, \sigma)$ where $G(s, \sigma) = \frac{1}{2}(U^+ + U^-)$ (s, σ). These solutions can be expressed in terms of Hermite polynomials. The conservation of the total heat implies the duality relation:

$$\int_{-\infty}^{+\infty} ds G(s, \sigma) = \int_0^\infty ds \frac{1}{\pi} \text{Im}\Pi(s) = \int_0^\infty ds U^+(s, \sigma), \quad (49.32)$$

where the last equality comes from the symmetry properties of $U^+(s, \sigma)$. A relation involving higher moments of the spectral function can also be deduced using the generating function of Hermite polynomials and leads to the sum rules:

$$\begin{aligned} \sigma^n \int_0^\infty ds H_{2n} \left(\frac{s}{2\sqrt{\sigma}}\right) U^+(s, \sigma) &= \int_0^\infty dt t^{2n} \frac{1}{\pi} \text{Im}\Pi(t), \\ \sigma^{n+1/2} \int_0^\infty ds H_{2n+1} \left(\frac{s}{2\sqrt{\sigma}}\right) U^-(s, \sigma) &= \int_0^\infty dt t^{2n+1} \frac{1}{\pi} \text{Im}\Pi(t), \end{aligned} \quad (49.33)$$

which only become useful once statements about the restriction to finite intervals can be made. In this case, Eq. (49.33) leads to the FESR in Eq. (49.15).

In [405,361], the example of the ρ meson has been taken for illustrating the Gaussian sum rules and summarized in the following figures. Figure 49.4 shows the evolution in the pseudo-‘time’ variable σ of the Gaussian transform of the spectral function *ansatz*

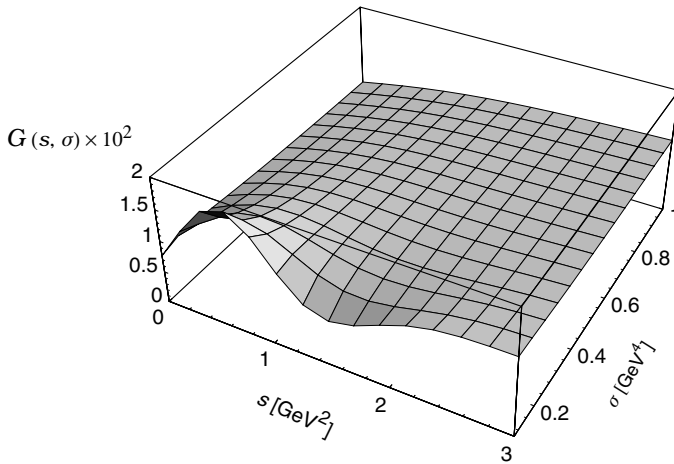


Fig. 49.4. The Gaussian transform of the spectral function in Eq. (49.18).

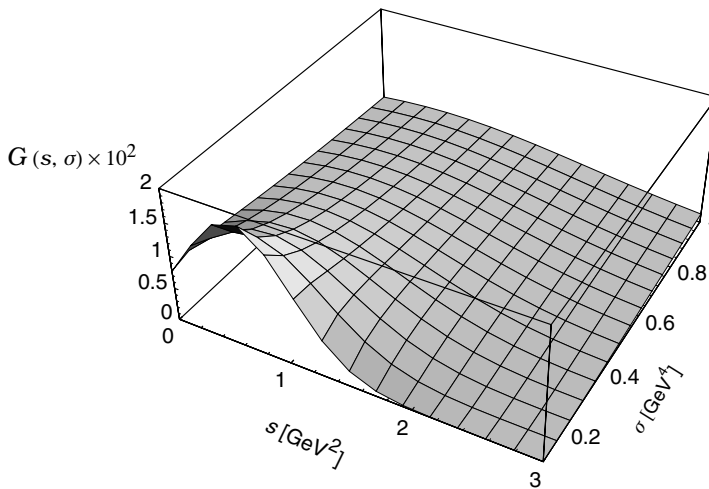


Fig. 49.5. The Gaussian transform of the spectral function in Eq. (49.35).

in Eq. (49.18) with the onset of the continuum t_c fixed by the finite energy sum rule in Eq. (49.19).

In the ‘heat evolution’ analogy the spectral function in Eq. (49.18) corresponds to the initial ‘heat distribution’ in the s -axis. The picture shows the evolution in ‘time’ of this ‘heat distribution’ in the interval $0.1 \text{ GeV}^4 \leq \sigma \leq 1 \text{ GeV}^4$. We observe that asymptotically in ‘time’, i.e. for σ large, the spectral function evolves very well to the asymptotic ‘heat distribution’ predicted by pQCD i.e.:

$$\lim_{\sigma \rightarrow \infty} G(s, \sigma) = \frac{1}{16\pi^2} \left(1 - \text{erf} \left(\frac{s}{2\sqrt{\sigma}} \right) \right) [1 + \dots], \quad (49.34)$$

where $\text{erf}(x)$ denotes the error function $\text{erf}(x) = \frac{2}{\sqrt{\pi}} \int_0^x dy e^{-y^2}$. By contrast, Fig. 49.5 shows

the same evolution in the limit case of only a delta-function *ansatz* for the spectral function:

$$\frac{1}{\pi} \text{Im}\Pi_{I=1}(t) = f_\rho^2 M_\rho^2 \delta(t - M_\rho^2), \quad (49.35)$$

with no continuum.

Clearly the corresponding asymptotic ‘heat distribution’ fails to reproduce the shape predicted by pQCD. *Global duality* of a given hadronic spectral function *ansatz* with QCD is only obtained provided that the hadronic parameters are constrained to satisfy a system of finite-energy sum rules equations.

49.7 FESR from the zeta prescription

Finally, the last (but not the least) way of deriving Eq. (49.15) is simply to take the coefficient of the τ variable in the two sides of the LSR in Eq. (49.7) [629,667]. This latter method can be formalized by using the zeta function prescription inspired from the non-relativistic approach [406]. In fact, if H is a Hamilton operator, the associated zeta-function can be written as:

$$\zeta(n) = \frac{1}{\Gamma(n)} \int_0^\infty dt \tau^{n-1} \text{Tr} e^{-Ht}, \quad (49.36)$$

which is equivalent, in field theory, to:

$$\zeta(n) = \frac{1}{\Gamma(n)} \int_0^\infty dt e^{-t\tau} \frac{1}{\pi} \text{Im}\Pi(t), \quad (49.37)$$

where the last integral is the familiar Laplace transform of $\text{Im}\Pi(t)$. If this Laplace-transform and its successive derivatives are a series in τ , then, one can easily derive Eq. (49.15) by comparing the exact expression of $\zeta(n=0)$ with its approximate form.

49.8 Analytic continuation

Various versions of this method have been discussed in the literature [630]. In most cases, the problem is formulated in terms of norm problems for the input errors and is quite similar to the standard χ^2 -minimization used in numerical analysis. More explicitly let us take a simple example. A polynomial in t is used for approximating the $1/(t - q^2)$ term of Eq. (48.2) in the real axis [630]. Then, applying the Cauchy theorem to the finite Q^2 contour in the complex Q^2 plane, one arrives at the sum rule:

$$\begin{aligned} \Pi(q^2) &= \frac{1}{2i\pi} \oint_C dt \left(\frac{1}{t - q^2} - \sum_{a_n} t^n \right) \Pi(t) \\ &+ \left[\Delta_n \equiv \frac{1}{\pi} \int_0^{Q^2} dt \left(\frac{1}{t - q^2} - \sum_n a_n t^n \right) \right] \text{Im}\Pi(t), \quad (49.38) \end{aligned}$$

where Δ_n is the ‘fit error’ which should tend to zero, if the result is optimal. An important difference with the previous sum rules is that in the RHS the data enters only in Δ_n whilst

the main part of $\Pi(q^2)$ is given by its theoretical side. However, it is difficult to appreciate the reliability of the results coming from the method due to:

- The *ad hoc* uses of the polynomial parametrization (or in general of the kernels in the integrals) and to the strong dependence of the results on the values of the input errors.
- Its form in Eq. (49.38) where the dependence of the sum rule on the arbitrary subtraction scale is unclear.
- The way of extrapolating the QCD information up to small q^2 which is model dependent.

Due to these weak points, all the beautiful mathematical forms used to formulate the sum rule might lose their efficiency in its physical applications. More refinements and more phenomenological tests of this approach are needed before a definite claim about its superiority can be made.

49.9 Summary

We have given a brief general survey of spectral function sum rule methods which we believe can be applied for a general class of QCD-like theories. As one can see all the methods presented here have their own advantages and disadvantages. For the particular case of QCD where the theory has not yet been solved exactly, some questions, though important, such as the existence of high derivatives at high Q^2 as well as a correct and convincing way of estimating the true theoretical systematic errors in the sum rules analysis remain academic. We have checked in a QCD-like model such as the non-linear σ model in two dimensions, as suggested by Gabriele Veneziano, that the high derivatives for a two-point correlator exist unambiguously. Also, one can always test a posteriori whether the assumptions used for the analysis make sense.

In this review, we shall mainly concentrate on the uses of the LSR in Eq. (49.7) to Eq. (49.9) owing to their sensitivity with respect to the low-energy behaviour of the spectral functions. However, in most cases, we shall also discuss for a comparison, the constraints from FESR in Eq. (49.15) which complement the LSR results.

49.10 Optimization criteria

One can notice that the sum rule variables τ (LSR variable) or n (finite number of derivatives) and the continuum threshold t_c are, in general, free parameters in the sum rule analysis.

- In the original work of SVZ [1], the optimal result from the sum rule is obtained inside a window in τ or n , where one has a balance between the QCD continuum and the non-perturbative condensates contributions in the sum rule. In QSSR1 [3], one has shown that this feature corresponds to the existence of a minimum in τ or n , as can be illustrated by the example of three-dimensional harmonic oscillator in quantum mechanics and of the charmonium sum rules [91–93].

49.10.1 The harmonic oscillator

For this purpose, let consider the harmonic oscillator potential:

$$V(r) = \frac{1}{2}m\omega^2 r^2, \quad (49.39)$$

and the ‘correlation function’ for the S -wave states:

$$F(\tau) = \sum (R_n)^2 e^{-E_n \tau} : \quad n = 0, 2, 4, \dots, \quad (49.40)$$

where R_n is the radial wave function for zero angular momentum and E_n the corresponding eigenvalue. τ is the parameter which regulates the energy resolution of the sum rule and plays the role of an ‘imaginary time’ variable. The exact solution of the LHS for the harmonic oscillator potential $V(r)$ reads:

$$F(\tau)_{\text{exact}} = \frac{2}{\sqrt{2\pi}} \left(\frac{m\omega}{\sinh \omega\tau} \right)^{3/2}, \quad (49.41)$$

where one can see that, in the limit $\tau \rightarrow \infty$, the exact expression:

$$\mathcal{R}(\tau)_{\text{exact}} \equiv -\frac{d}{d\tau} \log F(\tau) \quad (49.42)$$

tends to the lowest eigenvalue:

$$E_0 = \frac{3}{2}\omega. \quad (49.43)$$

At finite τ and for a truncated series in τ , one can write the approximate solution:

$$\mathcal{R}(\tau)_{\text{approx}} \equiv E_0 \left[\frac{1}{\omega\tau} + \frac{\omega\tau}{3} - \frac{(\omega\tau)^3}{45} + \frac{2(\omega\tau)^5}{945} + \dots \right], \quad (49.44)$$

where the first term is the free motion, and the next ones are higher-order corrections in τ to this term. One can notice that in this approximate solution, one cannot take formally the limit $\tau \rightarrow \infty$, as the asymptotic series will blow up. Therefore, a comparison of the exact and approximate solution can only be done in a compromise region where the series converge and where the S states contribution is dominant. This is exactly the situation which we shall encounter in the QCD sum rule analysis. The τ behaviour of $\mathcal{R}_{\text{approx}}(\tau)$ is shown in the Fig. 49.6, which one can compare with the eigenvalue E_0 . One can notice that it stays above E_0 as a consequence of the positivity of \mathcal{R} . The agreement between $\mathcal{R}_{\text{approx}}$ and $\mathcal{R}_{\text{exact}}$ increases if one adds more and more terms in the τ expansion. The minimum of $\mathcal{R}_{\text{approx}}$ provides an upper bound to the value of E_0 while the distance between $\mathcal{R}_{\text{approx}}$ and E_0 controls the strength of the continuum contribution to the sum rule. One can notice that the optimal information from $\mathcal{R}_{\text{approx}}$ is obtained at the minimum, where there is a balance between the higher order terms in the expansion and the higher states contributions.

We shall see that this quantum mechanics example mimics quite well the case of QCD.

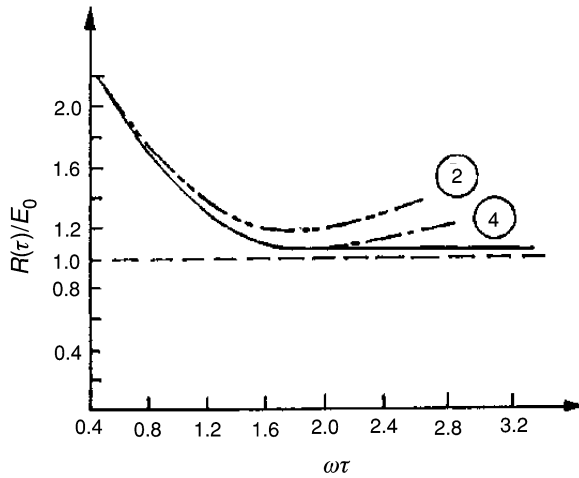


Fig. 49.6. The ratio of moments normalized to the ground-state energy versus the imaginary time for the case of the harmonic oscillator potential. (2) and (4): approximate series including the second and fourth order terms; — — — exact solution.

49.10.2 Non-relativistic charmonium sum rules

Retaining the correction due to the gluon condensate, the QCD expression of the non-relativistic QCD moments is [91–93]:

$$\begin{aligned} \mathcal{M}(\tau_N) &\equiv \int dE e^{-E\tau_N} \text{Im}\Pi(E) \\ &= \frac{3}{8m^2} 4\pi \left(\frac{m}{4\pi\tau_N} \right)^{3/2} \left[1 + \frac{4}{3} \alpha_s \sqrt{\pi m} \tau_N^{1/2} - \frac{4\pi}{288m} \langle \alpha_s G^2 \rangle \tau_N^3 \right], \end{aligned} \tag{49.45}$$

where τ_N is the imaginary time variable, from which one can deduce the ratio of moments:

$$\mathcal{R}(\tau_N) = \frac{3}{2\tau_N} - \frac{2}{3} \alpha_s \sqrt{\pi m} \tau_N^{-1/2} + \frac{4\pi}{96m} \langle \alpha_s G^2 \rangle \tau_N^2, \tag{49.46}$$

where m is the charm quark (pole) mass. Using the QCD parameters given in Tables 48.1 and 48.2, one can show in Fig. 49.7 the τ_N behaviour of the ratio of moments. One can notice a strict resemblance with the case of the harmonic oscillator.

The moments have the following features:

- The exact ratio reaches its limit E_0 very quickly as shown in Fig. 49.7.
- The theoretical curve which is a good approximation for small times stabilizes at medium time and blows up at large time indicating a breaking of the approximation for $\tau_N \geq \tau_N^c$. At the minimum, one has:

$$\min \mathcal{R}(\tau_N^c) = E_0^{\text{exact}} \tag{49.47}$$

within about 10% accuracy, indicating a good description of the ground state energy. This slight

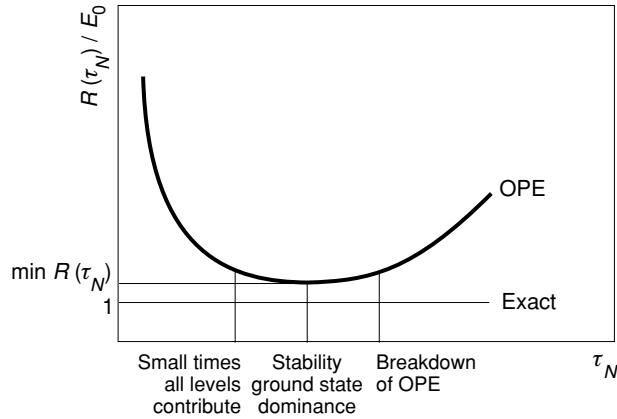


Fig. 49.7. The ratio of moments normalized to the ground-state energy versus the imaginary time in the case of the charmonium sum rules.

discrepancy can be reduced by including the contribution of the QCD continuum into the spectral function.

- However, it is quite surprising that, for a clearly emerging level where one would expect a dominance of the confinement force, while the moment shows that there exists a window where perturbation theory still works but the individual energy levels clearly emerge. For this reason, Bell–Bertlmann called it *magic moments*.

49.10.3 Implications for QCD

- However, by working with a truncated series as in QCD, we do not often have, in some other channels, a nice minimum for $\mathcal{R}_{\text{approx}}$. This minimum is replaced in some cases by an inflexion point where the optimal information on the resonance properties is obtained.
- Moreover, we need also a similar optimization for the value of the QCD continuum threshold t_c , which, a priori, is also a free parameter. Optimal estimate can be obtained if the result presents stability in t_c . In various examples, this procedure can lead to an overestimate of the result, such that one can safely consider the result obtained in this way as an upper bound. On the contrary, a lower bound can be obtained at the value of t_c where one starts to have a minimum or an inflexion point with respect to the changes of the sum rule variables τ or n . A further test of the t_c value is its comparison with the one obtained from FESR constraints.
- We conclude from the previous analysis that the optimal and most conservative results from the sum rule discussed in this book will obey the τ or n optimization criterion (SVZ window), but in addition the corresponding t_c values are in the range where we start to have these τ or n minimum until the one where we have a stability in t_c . In many examples, the value of t_c from a FESR constraint belongs to this range. In some cases, t_c can be higher than the value intuitively expected around the mass of the radial excitation, which is not very surprising as the QCD continuum is an average of all the higher-state contributions. Finally, one can also test that at the optimal region, the OPE still makes sense as the QCD series converge quite well.

49.11 Modelling the $e^+e^- \rightarrow I = 1$ hadrons data using a QCD-duality ansatz

Due to the complexity and to the absence of the data in some channels, it appears necessary to introduce a simple model for parametrizing the spectral function. In the example of the ρ meson, we have used the parametrization:

$$\frac{1}{\pi} \text{Im}\Pi_\rho(t) = \frac{M_\rho^2}{4\gamma_\rho^2} \delta(t - M_\rho^2) + \Theta(t - t_c) \text{ 'QCD continuum' }, \quad (49.48)$$

where the first term is the lowest resonance contribution, whilst the second one takes into account *all* discontinuities coming from the QCD diagrams. γ_ρ is the ρ -meson coupling to the vector current:

$$V_\mu = \frac{1}{2}(\bar{u}\gamma_\mu u - \bar{d}\gamma_\mu d), \quad (49.49)$$

and is normalized as in Eq. (2.52). We have also seen that the lowest FESR moment leads to the constraint:

$$\frac{M_\rho^2}{4\gamma_\rho^2} \simeq \frac{t_c}{8\pi^2} \left[1 + \left(\frac{\alpha_s}{\pi} \right) + \mathcal{O}(\bar{\alpha}_s^2) \right], \quad (49.50)$$

which, given the experimental value $\gamma_\rho \simeq 2.55$, leads to:

$$t_c \simeq 1.7 \text{ GeV}^2. \quad (49.51)$$

As first noticed in [405], this FESR constraint shows that the properties of the lowest ground state is correlated to the value of the QCD continuum threshold, and permits one to check the (in)consistencies of various predictions done in the early literature on the sum rules.

We compare the prediction of this model with the available complete $e^+e^- \rightarrow I = 1$ hadrons data for the ratio of moments $\mathcal{R}(\tau)$ as shown in Fig. 49.8.²

We have used the e^+e^- total cross-section shown in Fig. 49.9.

One can notice that the deviation of this *naïve and simple model* (dashed curve) from the data (black points) is at most 15%,³ and that is very good. One can also notice that the QCD duality ansatz prediction is below the complete data one, which can be understood because the QCD continuum might give an underestimate of the radial excitation contributions as it only gives a smearing of the higher-state effects and does not account for the complex resonance structure between 1 and 2 GeV.

49.12 Test of the QCD-duality ansatz in the charmonium sum rules

Let us now test the validity of the QCD-duality ansatz in the heavy quark sector. In so doing, we consider the charmonium family (J/ψ , ψ' , ...), which couples to the charm current

² More details discussions can be found in QSSR1 [3].

³ The continuous curve corresponds to another set: $\gamma_\rho = 2.2$ and $t_c = 2.2 \text{ GeV}^2$, which gives a worse prediction.

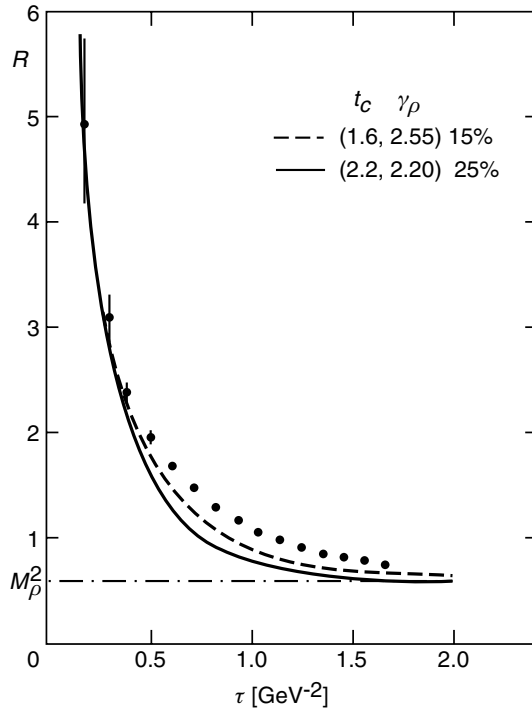


Fig. 49.8. Ratio of moments $\mathcal{R}(\tau)$ as function of the sum rule variable τ in the ρ -meson channel for two values of t_c and γ_ρ . The data points are $e^+e^- \rightarrow I = 1$ hadrons.

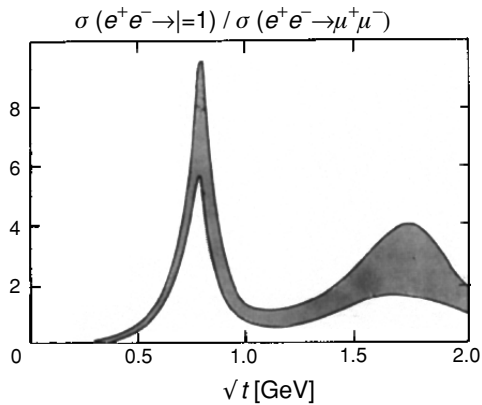


Fig. 49.9. Ratio of the $e^+e^- \rightarrow I = 1$ hadrons over the $e^+e^- \rightarrow \mu^+\mu^-$ total cross-section as function of the c.o.m energy \sqrt{t} .

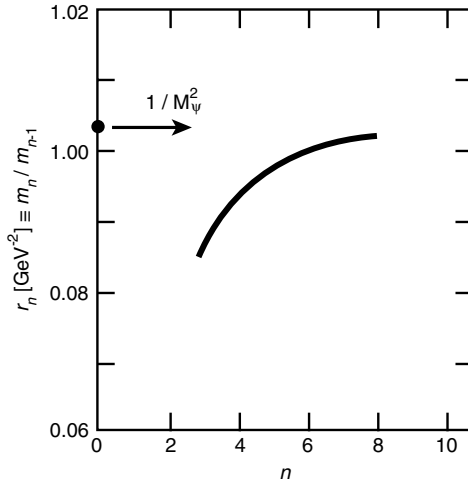


Fig. 49.10. Phenomenological side of the ratio of moments versus n .

via:

$$\langle 0 | \bar{c} \gamma^\mu c | \psi \rangle = \sqrt{2} \frac{M_\psi^2}{2\gamma_\psi} \epsilon^\mu, \tag{49.52}$$

and the corresponding two-point correlator. The coupling γ_ψ is normalized as in Eq. (1.51). The QCD continuum is simply approximated by the step function:

$$\frac{1}{\pi} \text{Im} \Pi_\psi(t)_{\text{cont}} = \frac{1}{4\pi^2} \left[1 + \left(\frac{\alpha_s}{\pi} \right) (t) \right] \Theta(t - t_c), \tag{49.53}$$

which one can improve by including the available quark mass and higher-order radiative corrections. We show in Fig. 49.10 the ratio of the $Q^2 = 0$ moments:⁴

$$r_n \equiv \frac{\mathcal{M}_n}{\mathcal{M}_{n-1}}, \tag{49.54}$$

by using the data for the different leptonic widths of the J/ψ family and by including the QCD continuum. One can notice that for larger value of $n \geq 6$, the ratio of moments is completely saturated by the lowest mass resonance, which shows that the QCD duality ansatz parametrization is a good approximation in the sum rule analysis of the heavy quark sector.

49.13 HQET sum rules

QCD spectral sum rules are often used in the Heavy Quark Effective Theory (HQET) for the estimate of meson masses and decay constants [164]. One considers the correlation

⁴ More detailed discussions can be found in QSSR1 [2].

functions of quark currents, where the heavy quarks are represented by their effective fields $h_v(x)$, v being the heavy quark four-velocity. For this purpose, let's consider the two-point correlation function:

$$\Pi(\omega) = i \int d^4x e^{ik \cdot x} \langle 0 | T \{ J_H(x) J_H^\dagger(0) \} | 0 \rangle \quad (49.55)$$

where $\omega = 2v \cdot k$ and $J_H(x) = \bar{h}_v(x) i \gamma_5 q(x)$ is the interpolating current of the pseudoscalar heavy-light mesons in HQET. In HQET, the corresponding decay constant f_B can be expressed in terms of the parameter \hat{F} as:

$$f_B = \hat{C}(m_b) \hat{F} \left[1 - \frac{A}{m_b} + \mathcal{O}\left(\frac{1}{m_b^2}\right) \right], \quad (49.56)$$

where the coefficient $\hat{C}(m_b)$ can be computed in perturbation theory. One can notice that due to the heavy quark spin symmetry, \hat{F} can also be computed from the two-point correlation function of the vector currents $J_V(x) = \bar{h}_v(x) (\gamma_\mu - v_\mu) q(x)$ interpolating heavy-light 1^- mesons. Isolating the ground state contribution from the integral over the excited states and the continuum, one can write the dispersion relation:

$$\Pi(\omega) = \frac{\hat{F}^2}{2\bar{\Lambda} - \omega} + \int_{E_0}^{\infty} dE \frac{\text{Im}\Pi(E)}{E - \omega} + \text{subtractions} . \quad (49.57)$$

The variable E is related to the usual t variable as:

$$t = (E + m_b)^2 . \quad (49.58)$$

The parameter $\bar{\Lambda} \simeq M_B - m_b$ represents the binding energy of the light degrees of freedom in the heavy meson. Here m_b represents the heavy quark pole mass. The dispersion relation, Eq. (49.57), is then matched with the QCD expression, obtained for negative ω using the SVZ expansion:

$$\Pi(\omega) = \Pi_{\text{pert}}(\omega) + \sum_d C_d \frac{\langle O_d \rangle}{(-\omega)^d} . \quad (49.59)$$

It is also convenient in the Laplace sum rule analysis to introduce the non-relativistic variable:

$$\tau_N = 4m_b \tau . \quad (49.60)$$

49.13.1 Decay constant, meson-quark mass gap, kinetic energy and chromomagnetic operator

Different applications of this method to the two-point functions of heavy-light meson and baryon currents have been focused on the estimate of the decay constant, the hadron-quark mass gap $\bar{\Lambda}$, the kinetic energy λ_1 and the chromomagnetic interaction parameter λ_2 .

The value of the B meson decay constant obtained from the analysis is [164,166]:

$$\hat{F} = (0.4 \pm 0.06) \text{ GeV}^{3/2}, \quad A = (0.9 \pm 0.2) \text{ GeV}, \quad (49.61)$$

which one can compare with the result obtained from the full theory discussed later on in the chapter of quark masses and decay constants.

The meson-quark mass gap $\bar{\Lambda}$ is an important input in HQET approach. Recall (see previous chapter on HQET) that it can be defined as [164,166]:⁵

$$M_{H_Q} = m_Q + \bar{\Lambda} + \frac{\Delta m^2}{2m_Q}, \quad (49.62)$$

with:

$$\Delta m^2 = -\lambda_1 + 2 \left[J(J+1) - \frac{3}{2} \right] \lambda_2, \quad (49.63)$$

$J = j \pm 1/2$ being the total spin of the hadron states. Taking, for definiteness, the case of the B meson, one has:

$$\lambda_1 \equiv \frac{1}{2M_B} \langle B(v) | \mathcal{O}_{\text{kin}} | B(v) \rangle \quad \text{and} \quad \lambda_2 \equiv -\frac{1}{3M_B} \langle B(v) | \mathcal{O}_{\text{mag}} | B(v) \rangle \quad (49.64)$$

which correspond respectively to the matrix elements of the kinetic and of the chromomagnetic operators:

$$\mathcal{O}_{\text{kin}} \equiv \bar{h}(iD)^2 h \quad \text{and} \quad \mathcal{O}_{\text{mag}} \equiv \frac{1}{4} g_s \bar{h} \sigma_{\mu\nu} G^{\mu\nu} h, \quad (49.65)$$

where h is the heavy quark field and $G^{\mu\nu}$ the gluon field strength tensor.

The estimate of $\bar{\Lambda}$ from HQET-sum rules leads to [165]:

$$\bar{\Lambda} \simeq (0.52 - 0.70) \text{ GeV}, \quad (49.66)$$

in good agreement with the previous results [164,633], although less accurate as we have taken a larger range of variation for the continuum energy. An analogous sum rule in the full QCD theory leads to [634]:

$$\bar{\Lambda} \simeq (0.6 - 0.80) \text{ GeV}, \quad (49.67)$$

which combined together leads to the intersecting range of values [165]:

$$\bar{\Lambda} \simeq (0.65 \pm 0.05) \text{ GeV}. \quad (49.68)$$

The sum rule estimate of the kinetic energy gives [165]:

$$\lambda_1 \simeq -(0.5 \pm 0.2) \text{ GeV}^2 \quad (49.69)$$

where the large error, compared with the previous result of [166], is due to the absence of the stability point with respect to the variation of the continuum energy threshold. By

⁵ We are aware of the fact that in the lattice calculations, $\bar{\Lambda}$ defined in this way can be affected by renormalons [798].

combining the previous estimates with the one of the chromomagnetic energy:

$$\lambda_2 \simeq \frac{1}{4}(M_{B^*}^2 - M_B^2) + \mathcal{O}(1/m_b) \simeq 0.49 \text{ GeV}^2, \quad (49.70)$$

one deduces the value of the pole mass to two-loop accuracy:

$$M_b \equiv m_b = (4.61 \pm 0.05) \text{ GeV}, \quad (49.71)$$

in good agreement with the previous values from the sum rules in the full theory and (within the errors) with the HQET results in [164,633].

49.13.2 Isgur–Wise function

This approach has been also extended to the three-point function for studying the Isgur–Wise function for the $B \rightarrow D^{(*)}$ semi-leptonic transition [164]. Compared with the sum rule in the full theory, the HQET sum rules have a much simpler QCD expression because it is a series in $1/M_b$. Therefore, the evaluation of radiative corrections like the one for the three-point function becomes feasible. We shall come back to this point in the chapter on B and D exclusive weak decays.

49.14 Vertex sum rules and form factors

The extension of QSSR two-point function sum rules into vertex or three-point function sum rules has been discussed by many authors [635–641] and in many reviews on sum rules [356–365], with the aim of estimating the three-hadron couplings and to study the q^2 -dependence of the hadron form factors. In most of these applications, the vertex is saturated by the lowest hadronic state plus a QCD continuum, while the QCD expressions are evaluated in the Euclidian region using a configuration that is best suited to the processes considered. The mathematical validity of the spectral representation for the three-point function is not well established in general,⁶ although one may expect that, in the case of narrow resonances, it simplifies, due to the disappearance of some anomalous thresholds.⁷ Among other choices, the symmetric configuration:

$$p^2 = q^2 = (p + q)^2 = -(Q^2 \gg \Lambda^2), \quad (49.72)$$

for the vertex depicted in Fig. 49.11 appears to be convenient for extracting the trilinear boson couplings, as we are only left with one variable in the sum rule analysis, while its QCD side is guaranteed to be safe from some eventual IR singularities. In this narrow-width approximation, one can write the duality diagrams between the two sides of the vertex sum rules (Fig. 49.12).

⁶ To our knowledge, the most serious attempts to study such a problem is in [640] within perturbation theory.

⁷ Related discussions will be done in the next chapter, taking the example of the B_c meson semi-leptonic decays.

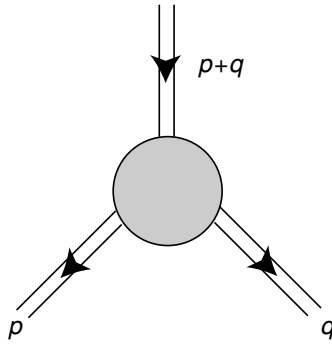


Fig. 49.11. Hadronic vertex.

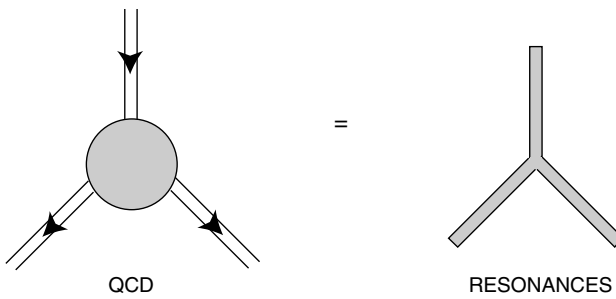


Fig. 49.12. Duality between a QCD vertex and a hadronic vertex in a narrow width approximation.

The discussions on the theoretical validity of the symmetric configuration method and its first phenomenological applications in QCD, for the case of trilinear mesons [637] and meson-baryon-baryon couplings, can be found in [636]. Some other applications of this method will be discussed later on in following chapters for the estimate of the decay widths of scalar mesons, gluonia and hybrids. The case of the heavy meson exclusive decays will be extensively discussed.

The uses of vertex sum rules for studying the q^2 -dependence of different light and heavy hadron form factors have been also discussed extensively in the literature and will be discussed in later chapters. In connection to this, we shall also discuss light-cone sum rules that are an alternative to the vertex sum rules.

49.14.1 Spectral representation

The hadronic vertex in Fig. 49.11, can be represented by the spectral representation:

$$T(p^2, q^2, (p + q)^2) = \frac{1}{\pi} \int dt_1 dt_2 dt_3 \frac{\text{Im}T(t_1, t_2, t_3)}{(t_1 - p^2)(t_2 - q^2)(t_3 - (p + q)^2)}. \quad (49.73)$$

In the symmetric representation given in Eq. (49.72), it takes the simple form:

$$T(Q^2) = \frac{2}{\pi} \int_0^1 x dx \int_0^1 dy \int_0^\infty dt_1 dt_2 dt_3 \frac{\text{Im}T(t_1, t_2, t_3)}{[Q^2 + (t_1 - t_2)xy + (t_2 - t_3)x + t_3]^3}, \tag{49.74}$$

after a Feynmann parametrization of the propagators. In this form, it is trivial to apply the Laplace sum rule operator for improving the duality relation. One obtains:

$$\hat{\mathcal{L}}[T] = \frac{\tau^3}{\pi} \int_0^1 x dx \int_0^1 dy \int_0^\infty dt_1 dt_2 dt_3 e^{-[(t_1-t_2)xy+(t_2-t_3)x+t_3]\tau} \text{Im}T(t_1, t_2, t_3), \tag{49.75}$$

where the rôle of the depressive factor is only manifest when the mass of the first excited state is much higher than any of the lowest ground states involved in the three channels.

An alternative choice of configurations often used in the literature is to take one of the three-moment fixed or small. In this case, one assumes the validity of the double-dispersion relation:

$$T(q^2, p^2) = \int_0^\infty dt_1 \int_0^\infty dt_2 \frac{\text{Im}T(t_1, t_2, (p+q)^2)}{(t_1 - p^2)(t_2 - q^2)} + \dots \tag{49.76}$$

One can apply a double ‘Borel’ transformation for each variable p^2 and q^2 provided that the subtraction terms are not of the form [641]:

$$(p^2)^n \int_0^\infty \frac{\Delta(t)dt}{(t - q^2)} \quad \text{or} \quad (q^2)^n \int_0^\infty \frac{\Delta(t)dt}{(t - p^2)}, \tag{49.77}$$

which would induce non-controllable contributions to the sum rule. However, treating (p^2, q^2) as independent variables may not be justified, as the spectral representation should be done in a (q^2, p^2) plane along a straight-line which is a combination of the variables p^2 and q^2 [635].

49.14.2 Illustration from the evaluation of the $g_{\omega\rho\pi}$ coupling

The relevant three-point function is:

$$\begin{aligned} T_{\mu\nu}(p, q) &= i \int d^4x e^{-ip \cdot x} e^{i(p+q) \cdot y} \langle | \mathcal{T} J_\mu^\rho(x) J_\nu^\pi(y) J_\nu^\omega(0) | 0 \rangle \\ &= \epsilon_{\mu\nu\alpha\beta} p^\alpha q^\beta T(Q^2, (p - q)^2). \end{aligned} \tag{49.78}$$

where T is the invariant amplitude. The quark interpolating currents are normalized as:

$$J_\mu^\rho =: \bar{u} \gamma_\mu d : \quad J_\nu^\omega = \frac{1}{6} : \bar{u} \gamma_\nu u + \bar{d} \gamma_\nu d : \quad J^\pi = (m_u + m_d) : \bar{d}(i \gamma_5) u : . \tag{49.79}$$

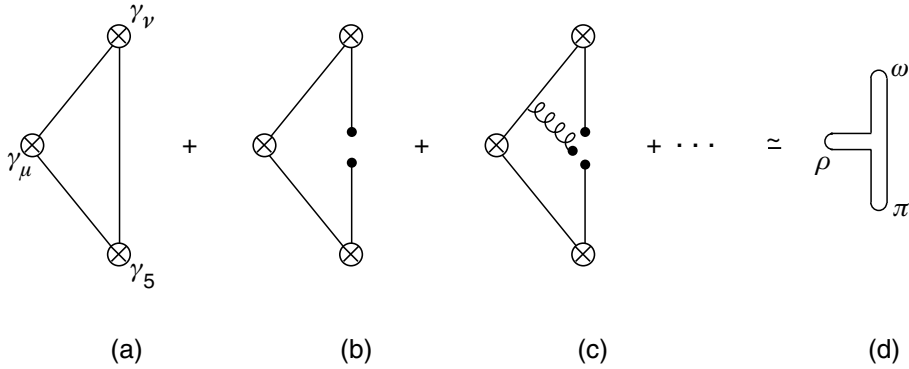


Fig. 49.13. Duality between the QCD and hadronic vertices for $g_{\omega\rho\pi}$: (a), (b) and (c) are respectively the QCD perturbative, quark condensate and mixed quark condensate contributions; (d) is the $g_{\omega\rho\pi}$ coupling.

The QCD expression of the vertex at the symmetric point can be evaluated from the diagrams depicted in Fig. 49.13 and gives [637]:

$$T(p, q) = \frac{1}{16\pi^2} \frac{(m_u + m_d)}{Q^2} \left\{ (m_u + m_d) I_{x,y} - \frac{\langle \bar{u}u \rangle}{Q^2} \left(1 + \frac{5}{36} \frac{M_0^2}{Q^2} \right) \right\}. \quad (49.80)$$

We have parametrized the mixed quark condensate effects by introducing the scale $M_0^2 \simeq 0.8 \text{ GeV}^2$. $I_{x,y}$ is a typical Feynman parameter integral:

$$I_{x,y} = \int_0^1 dx \int_0^{1-x} dy \frac{1}{x(1-x) + y(1-y) - xy} = 2.34. \quad (49.81)$$

Using a narrow width approximation (NWA) and retaining the lowest mass resonances, one obtains:

$$T_{\text{exp}} = \frac{\sqrt{2} f_\pi m_\pi^2}{Q^2 + m_\pi^2} \frac{\sqrt{2} M_\rho^2}{2\gamma_\rho} \frac{\sqrt{2} M_\omega^2}{2\gamma_\omega} |g_{\omega\rho\pi}|. \quad (49.82)$$

We have used the usual normalization:

$$\langle 0 | J^\pi | \pi \rangle = \sqrt{2} m_\pi^2 f_\pi, \quad \langle 0 | J_\mu^\rho | \rho \rangle = \sqrt{2} \frac{M_\rho^2}{2\gamma_\rho} \epsilon_\mu, \quad \langle 0 | J_\nu^\omega | \omega \rangle = \frac{M_\omega^2}{2\gamma_\omega} \epsilon_\nu. \quad (49.83)$$

The hadronic coupling is normalized as:

$$\langle \omega(p_1, \epsilon_1) | \rho(p_2, \epsilon_2) \pi(p_3) \rangle = |g_{\omega\rho\pi}| \epsilon_{\mu\nu\rho\sigma} \epsilon_1^\mu \epsilon_2^\nu p_1^\rho p_2^\sigma. \quad (49.84)$$

Invoking quark-hadron duality and taking the Laplace transform, one obtains in the chiral limit and for $\gamma_\omega \simeq 3\gamma_\rho$, $M_\rho \simeq M_\omega$:

$$|g_{\omega\rho\pi}| \simeq \frac{6\gamma_\rho^2 (m_u + m_d) \langle \bar{u}u \rangle}{M_\rho^4 f_\pi m_\pi^2} \tau^{-1} e^{M_\rho^2 \tau} \left(1 + \frac{5}{36} M_0^2 \tau \right). \quad (49.85)$$

One can eliminate the quark condensate contribution using the GMOR relation:

$$(m_u + m_d)\langle\bar{u}u\rangle = -f_\pi^2 m_\pi^2. \quad (49.86)$$

However, one should not take literally the f_π dependence of the result as the f_π dependence of τ is not known. Using $\gamma_\rho = 2, 55$, it leads at the stability point $\tau \simeq 1.4 \text{ GeV}^{-2}$ to:

$$|g_{\omega\rho\pi}| \approx 19 \text{ GeV}^{-1} \quad (49.87)$$

in satisfactory agreement with the phenomenological determination of about 17 GeV^{-1} from $\omega \rightarrow 3\pi$ or $\omega \rightarrow \pi^0\gamma$ decay using the Gell–Sharp–Wagner model [642]. One should notice that even at these large τ -values, the contribution of the mixed condensate is only about 15% indicating the convergence of the OPE. The effect of radial excitations have also been shown [637] to be negligible.

Similar approaches have been used in some other channels [636,3] (see also forthcoming chapters).

49.15 Light-cone sum rules

49.15.1 Basics and illustration by the $\pi^0 \rightarrow \gamma^*\gamma^*$ process

The method of light-cone sum rules (LCSR) [643] is an alternative to the vertex sum rules for studying hadronic form factors.⁸ It combines the SVZ technique and the theory of hard exclusive processes [644]. The basic idea is to expand the products of currents near the light cone. It can be illustrated by the analysis of the pion form factor in the process $\pi^0 \rightarrow \gamma\gamma$ for on-shell pion ($p^2 = m_\pi^2 = 0$) in the chiral limit. The corresponding amplitude, is:

$$\begin{aligned} T_{\mu\nu}(p, q) &= i \int d^4x e^{-iq \cdot x} \langle \pi^0(p) | T J_\mu^{\text{em}}(x) J_\nu^{\text{em}}(0) | 0 \rangle \\ &= \epsilon_{\mu\nu\alpha\beta} p^\alpha q^\beta F(Q^2, (p-q)^2), \end{aligned} \quad (49.88)$$

where p is the pion momentum, q and $(p-q)$ are the photon momenta, $Q^2 = -q^2$, J_μ^{em} is the quark electromagnetic current and F is the invariant amplitude. To derive the LCSR, one has to calculate the correlation function of Eq. (49.88) in QCD, in the region of large Q^2 and $|(p-q)^2|$ and to use a dispersion relation to match the result of this calculation with hadronic matrix elements:

$$T_{\mu\nu}(p, q) = \frac{1}{\pi} \int_{s_0^h}^{\infty} ds \frac{\text{Im} T_{\mu\nu}(Q^2, s)}{s - (p-q)^2}. \quad (49.89)$$

The spectral function can be saturated by the lowest masses ρ and ω mesons via:

$$\langle V | J_\nu^{\text{em}}(0) | 0 \rangle = \epsilon_\nu \sqrt{2} \frac{M_V^2}{2\gamma_V} : \quad V \equiv \rho, \omega. \quad (49.90)$$

⁸ Various recent applications of this method are reviewed in [360].

The correlation function in Eq. (49.88) can be calculated by expanding the T product of quark currents near the light cone $x^2 = 0$, which, for large Q^2 and $|(p - q)^2|$, is expected to give the dominant contribution. This expansion is different from the local OPE as it no longer involves QCD vacuum condensates, but a summation of infinite series of local operators. It is convenient to introduce the DIS variables:

$$v \equiv p \cdot q, \quad \xi = 2v/Q^2. \tag{49.91}$$

The leading contribution to the amplitude can be obtained by contracting the quark fields ψ in Eq. (49.88), using the propagator of the free massless quark:

$$iS_0(x, 0) = \langle 0 | T\{\psi(x)\bar{\psi}(0)\} | 0 \rangle = \frac{i \not{x}}{2\pi^2 x^4}, \tag{49.92}$$

and transforming $\gamma_\mu \gamma_\alpha \gamma_\nu \rightarrow -i\epsilon_{\mu\alpha\nu\rho} \gamma^\rho \gamma_5 + \dots$. Then, one obtains:

$$T_{\mu\nu}(p, q) = -i\epsilon_{\mu\nu\alpha\rho} \int d^4x \frac{x^\alpha}{\pi^2 x^4} e^{-iq \cdot x} \langle \pi^0(p) | \bar{\psi}(x) \gamma^\rho \gamma_5 \psi(0) | 0 \rangle. \tag{49.93}$$

Expanding the local operators around $x = 0$:

$$\bar{\psi}(x) \gamma_\rho \gamma_5 \psi(0) = \sum_n \frac{1}{n!} \bar{\psi}(0) (\bar{D} \cdot x)^n \gamma_\rho \gamma_5 \psi(0), \tag{49.94}$$

the matrix elements of these operators have the following general decomposition:

$$\begin{aligned} \langle \pi^0(p) | \bar{\psi} \bar{D}_{\alpha_1} \bar{D}_{\alpha_2} \dots \bar{D}_{\alpha_r} \gamma_\rho \gamma_5 \psi | 0 \rangle &= (-i)^n p_{\alpha_1} p_{\alpha_2} \dots p_{\alpha_r} p_\rho M_n \\ &+ (-i)^n g_{\alpha_1 \alpha_2} p_{\alpha_3} \dots p_{\alpha_r} p_\rho M'_n + \dots, \end{aligned} \tag{49.95}$$

where M_n, M'_n are matrix elements coming respectively from twist-2 and twist-4 local operators. Substituting the decomposition Eq. (49.94) in Eq. (49.93), integrating over x and using the definitions Eq. (49.95) and Eq. (49.91) one obtains:

$$F(Q^2, (p - q)^2) = \frac{1}{Q^2} \sum_{n=0}^\infty \xi^n M_n + \frac{4}{Q^4} \sum_{n=2}^\infty \frac{\xi^{n-2}}{n(n-1)} M'_n + \dots \tag{49.96}$$

Since the variable $\xi \sim 1$ in a generic exclusive kinematics with $p \neq 0$, all terms should be kept in each series in this expression. The second term containing M'_n and further similar terms are suppressed by powers of a small parameter $1/Q^2$ as compared with the first term containing M_n . Keeping the lowest twist contribution, at $x^2 = 0$ (and $p^2 = 0$), the matrix element in Eq. (49.93) has the following parametrization ($f_\pi = 92.4$ MeV):

$$\langle \pi^0(p) | \bar{\psi}(x) \gamma_\mu \gamma_5 \psi(0) | 0 \rangle_{x^2=0} = -ip_\mu f_\pi \int_0^1 du e^{iup \cdot x} \varphi_\pi(u, \mu), \tag{49.97}$$

where the function $\varphi_\pi(u, \mu)$ is the pion *light-cone distribution amplitude* of twist 2, normalized to unity: $\int_0^1 \varphi_\pi(u, \mu) du = 1$. Furthermore, expanding both sides of Eq. (49.97) and comparing the LHS with the expansions, Eqs. (49.94) and (49.95), we find that the

moments of $\varphi_\pi(u)$ are related to the matrix elements of local twist-2 operators:

$$M_n = -i f_\pi \int_0^1 du u^n \varphi_\pi(u, \mu). \quad (49.98)$$

The function $\varphi_\pi(u)$, multiplied by f_π , is a universal non-perturbative object encoding the long-distance dynamics of the pion. Together with the corresponding higher-twist distribution amplitudes, $\varphi_\pi(u)$ plays a similar role as the vacuum condensates play in SVZ sum rules. However, to our opinion, a connection between the distribution amplitude and the vacuum condensates has not been yet clarified and needs further investigation. Substituting the definition Eq. (49.97) in Eq. (49.93), integrating over x , restoring the electromagnetic charge factor and summing the u and d quark contributions, one obtains the correlation function in the twist 2 approximation:

$$F^{(2)}(Q^2, (p-q)^2) = \frac{2}{3} f_\pi \int_0^1 \frac{du \varphi_\pi(u, \mu)}{\bar{u} Q^2 - u(p-q)^2}, \quad (49.99)$$

where $\bar{u} = 1 - u$. We are now in a position to obtain a sum rule from the dispersion relation, Eq. (49.89), matching it with the result of the light-cone expansion. We define the matrix element

$$\langle \pi^0(p) | j_\mu^{\text{em}} | \rho^0(p-q) \rangle = F^{\rho\pi}(Q^2) m_\rho^{-1} \epsilon_{\mu\nu\alpha\beta} \epsilon^{(\rho)\nu} q^\alpha p^\beta, \quad (49.100)$$

in terms of the transition form factor $F^{\rho\pi}(Q^2)$. We parametrize the higher state contributions by the QCD continuum ansatz from a threshold t_c and write a dispersion relation for $F^{(2)}$. It is easy to obtain, the duality relation, to leading twist-2 accuracy:

$$\frac{\sqrt{2} M_\rho}{2\gamma_\rho} \frac{F^{\rho\pi}(Q^2)}{m_\rho^2 - (p-q)^2} + \frac{1}{\pi} \int_{t_c}^\infty ds \frac{\text{Im} F(Q^2, s)}{s - (p-q)^2} = \frac{\sqrt{2} f_\pi}{3} \int_0^1 \frac{du \varphi_\pi(u)}{\bar{u} Q^2 - u(p-q)^2}, \quad (49.101)$$

where γ_ρ is the coupling normalized as usual in this book:

$$\langle 0 | \frac{1}{\sqrt{2}} (\bar{u} \gamma_\mu u - \bar{d} \gamma_\mu d) | \rho \rangle = \epsilon_\mu \frac{\sqrt{2} M_\rho^2}{2\gamma_\rho} \quad (49.102)$$

Introducing the continuum threshold:

$$u_c^\rho = Q^2 / (t_c + Q^2) \quad (49.103)$$

and taking the Laplace transform, one obtains the LCSR for the form factor of the $\gamma^* \rho \rightarrow \pi$ transition to twist-2 accuracy [645,360]:

$$F^{\rho\pi}(Q^2) = \frac{2}{3} \frac{f_\pi}{M_\rho} \gamma_\rho \int_{u_c}^1 \frac{du}{u} \varphi_\pi(u, \mu) \exp\left(-\frac{\bar{u} Q^2}{u M^2} + \frac{m_\rho^2}{M^2}\right). \quad (49.104)$$

$\rho \rightarrow \pi\pi$ form factor

Another example of the application of LCSR is the calculation of the pion electromagnetic form factor defined as:

$$\langle \pi(p') | j_\mu^{\text{em}} | \pi(p) \rangle = F_\pi(q^2)(p + p')_\mu, \tag{49.105}$$

where $q = p' - p$ and j_μ^{em} is the electromagnetic current:

$$j_\mu^{\text{em}} = e_u \bar{u} \gamma_\mu u + e_d \bar{d} \gamma_\mu d. \tag{49.106}$$

The resulting LCSR, at zeroth order in α_s and in the twist 2 approximation, reads [649]:

$$F_\pi(Q^2) = \int_{u_c^\pi}^1 du \varphi_\pi(u, \mu_u) \exp\left(-\frac{\bar{u} Q^2}{u M^2}\right) \xrightarrow{Q^2 \rightarrow \infty} \frac{\varphi'_\pi(0, M^2)}{Q^4} \int_0^{t_c^\pi} ds s e^{-s/M^2}, \tag{49.107}$$

where $\varphi'_\pi(0) = -\varphi'_\pi(1)$, and $u_c^\pi = Q^2/(t_c^\pi + Q^2)$, s_0^π is the duality threshold in the pion channel. The factorization scale $\mu_u^2 = \bar{u} Q^2 + u M^2$ corresponds to the average quark virtuality in the correlation function. At $O(\alpha_s)$, one recovers the leading $\sim 1/Q^2$ asymptotic behaviour corresponding to the hard scattering mechanism. Including this contribution in the LCSR and retaining the first two terms of the sum rule expansion in powers of $1/Q^2$ one obtains [650]:

$$F_\pi(Q^2) = \frac{2\alpha_s}{3\pi Q^2} \int_0^{s_0^\pi} ds e^{-s/M^2} \int_0^1 du \frac{\varphi_\pi(u)}{\bar{u}} + \varphi'_\pi(0) \int_0^{s_0} ds s \frac{e^{-s/M^2}}{Q^4} + O\left(\frac{\alpha_s}{Q^4}\right). \tag{49.108}$$

The $O(1/Q^2)$ term in Eq. (49.108) coincides with the well-known expression for the asymptotics of the pion form factor [644]:

$$F_\pi(Q^2) = \frac{8\pi\alpha_s f_\pi^2}{9Q^2} \left| \int_0^1 du \frac{\varphi_\pi(u)}{\bar{u}} \right|^2, \tag{49.109}$$

obtained by the convolution of two twist-2 distribution amplitudes $\varphi_\pi(u)$ of the initial and final pion with the $O(\alpha_s)$ quark hard-scattering kernel.

49.15.2 Distribution amplitudes

The model dependence and main uncertainties of the LCSR approach is in the parametrization of the distribution amplitude. It can be expanded using the conformal symmetry of massless QCD [360,646]. The conformal spin (partial wave) decomposition allows to represent each distribution amplitude as a sum of certain orthogonal polynomials in the variable u . The coefficients of these polynomials are multiplicatively renormalizable, and have growing anomalous dimensions, so that, at sufficiently large normalization scale μ , only the first few terms in this expansion are relevant. The part of the distribution amplitude, which does not receive logarithmic renormalization is called *asymptotic*. Within this

expansion, one can write:

$$\varphi_\pi(u, \mu) = 6u\bar{u} \left[1 + \sum_{n=2,4,\dots} a_n(\mu) C_n^{3/2}(u - \bar{u}) \right], \quad (49.110)$$

where $C_n^{3/2}$ are the Gegenbauer polynomials (for a derivation, see, e.g., [167]). The coefficients a_n are multiplicatively renormalizable:

$$a_n(\mu) = a_n(\mu_0) \left(\frac{\alpha_s(\mu)}{\alpha_s(\mu_0)} \right)^{\gamma_n/\beta_0}, \quad (49.111)$$

and:

$$\gamma_n = C_F \left[-3 - \frac{2}{(n+1)(n+2)} + 4 \left(\sum_{k=1}^{n+1} \frac{1}{k} \right) \right] \quad (49.112)$$

are the anomalous dimensions [647]. At $\mu \rightarrow \infty$, $a_n(\mu)$ vanish, and the limit $a_n = 0$ corresponds to the asymptotic distribution amplitude

$$\varphi_\pi^{(as)}(u) = 6u\bar{u}. \quad (49.113)$$

The values of the non-asymptotic coefficients a_n at a certain intermediate scale μ_0 can be estimated from two-point sum rules [647,648,3] for the moments $\int u^n \varphi_\pi(u, \mu) du$ at low n . This method is attractive because it employs non-perturbative information expressed in terms of quark and gluon condensates. However, in practice the two-point sum rule determination of a_n is not very accurate, such that one should consider conservatively the large range spanned by a_n from different analysis.